JOURNAL OF Materials CHEMISTRY

Molecular design of dopant precursors for atomic layer epitaxy of SrS : Ce†

William S. Rees, Jr.,* Oliver Just and Donald S. Van Derveer

School of Chemistry and Biochemistry and School of Materials Science and Engineering and Molecular Design Institute, Georgia Institute of Technology, Atlanta, GA 30332-0400, USA. E-mail: will.rees@chemistry.gatech.edu

Received 8th June 1998, Accepted 23rd July 1998

Two cerium compounds, $Ce\{N[Si(CH_3)_3]_2\}_3$ and $Ce(tmhd)_4$ (tmhd = 2,2,6,6-tetramethylheptane-3,5-dionate), have been evaluated for utilization in the preparation of thin films of SrS : Ce by atomic layer epitaxy (ALE). The resultant coatings have been characterized for use in electroluminescent (EL) devices. The observed emission maximum at 518 nm for the devices derived from $Ce(tmhd)_4$ shifts to 480 nm for those resulting from $Ce\{N[Si(CH_3)_3]_2\}_3$. This shift may be correlated with the basicity of the ligand present on the dopant element.

Introduction

For many years, monochrome electroluminescent (EL) devices have been available. The mass production of thin film EL (TFEL) structures is based on ZnS:Mn. This yellow visible light emitter is grown commercially by atomic layer epitaxy (ALE). The advantages of a TFEL approach over other competing flat panel display (FPD) technologies reside primarily in its combination of horizon-to-horizon undistorted field-of-view and its mechanical robustness. Although lighter weight, more energy efficient systems have been developed from alternative approaches, none have yet to emerge which possess the EL combination of ruggedness and viewability. Thus, it is of considerable interest to explore the potential of expansion of the TFEL approach to create full-color FPDs. Currently, several EL phosphors exist for choice among the color coordinates (Table 1); however, the most problematic component to date in this exciting field remains the search for a, as yet elusive, 'true' blue EL phosphor. Nevertheless, multicolor units have been prepared in the interim, until the challenges with a 'true' blue EL phosphor are met successfully.

In order to achieve satisfactory 'true' blue emission, a dual substrate approach has been adopted (Fig. 1). In this technique, SrS : Ce emission forms the dominant component of the blue region of the spectrum. In addition to the achievement of a color-faithful emission, other important criteria to address in this area include the emission efficiency and the brightness of the resultant display. Significant progress has been realized in these areas and they remain active research topics.[1–4]

ALE[5] emerged almost two decades ago as a most promising modification of the conventional MOCVD technique for fabrication of TFEL structures on glass substrates. The principle of the ALE process[6] (Fig. 2) is based on sequential interactions of the deposition surface with desired reactants, resulting in digitally controlled consecutive deposition of strictly defined single atomic layers at a time. Moderate deposition rates, and the potential of increased contamination effects, resulting from incomplete reaction cycles, which contribute to an enhanced rate of film defects; however, constitute certain limitations of this growth method. The key to note here is the difference between CVD and ALE. In CVD, the dominant growth process is activated thermally, whereas in ALE, primarily it is a protolytic event. This key difference is manifested in the design of precursors for the two processes. In conventional CVD, the thermal bond dissociation enthalpy is the figure of concern in removing ligands from the boundary layer above the actively growing substrate. In ALE, bond thermolysis plays a negligible role in film growth. Rather, the relative pK_a of the ligand on the alternating precursor gas inlet flows is the thermodynamic driving force for the reaction. Protonolysis of the conjugate base (L^-) liberates the free acid (HL), which, in turn, is fugitive from the reaction zone. The cycle repeats, as alternating sub-lattice layers of cation and anion are built up.

Table 1 Commonly employed EL phoshors and their properties

Phosphor material	Emission efficiency color	CIE[a] *x*	CIE *y*	L/ cd m^{-2}[b] @60 Hz	L W^{-1}[c]
ZnS : Mn	Yellow	0.50	0.50	300	3–6
CaS : Eu	Red	0.68	0.31	12	0.2
ZnS : Mn/ CdSSe filter	Red	0.65	0.35	65	0.8
ZnS : Tb	Green	0.30	0.60	100	0.6–1.3
SrS : Ce	Blue–green	0.30	0.50	100	0.8–1.6
$SrGa_2S_4$: Ce	Blue	0.15	0.10	5	0.02
$CaGa_2S_4$: Ce	Blue	0.15	0.19	10	0.03
SrS : Cu	Blue	0.16	0.24		
ZnS : Mn/ SrS : Ce	'White'	0.44	0.48	470	1.5

[a]1931 C.I.E. chromaticity diagram. [b]candelas meter^{-2}. [c]lumens watt^{-1}.

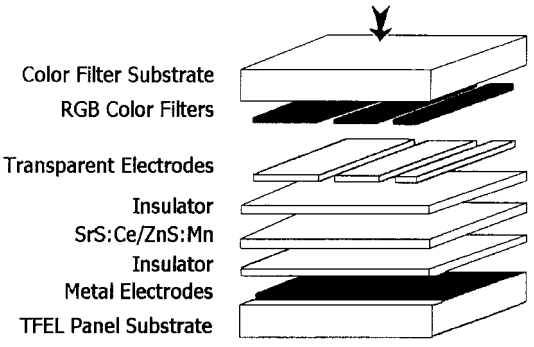

Fig. 1 Schematic illustration of dual-substrate EL devices.

†Basis of the presentation given at Materials Chemistry Discussion No. 1, 24–26 September 1998, ICMCB, University of Bordeaux, France.

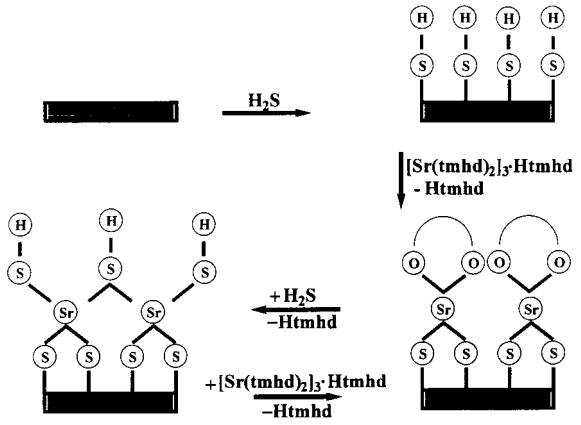

Fig. 2 Schematic representation of the atomic layer epitaxy (ALE) process.

Results and discussion

Following conventional ALE practices, TFEL structures of SrS:Ce were fabricated by Planar International in Helsinki, Finland. The sulfur source was H_2S, with a pK_{a1} of 7.04 and a pK_{a2} of 11.96.‡[7] The strontium source was 'Sr(tmhd)$_2$' with a pK_a(Htmhd) of 15.9.[8] It must be noted that 'Sr(tmhd)$_2$', *per se*, does not exist.[9] The most widely utilized anhydrous composition is [Sr(tmhd)$_2$]$_3$·Htmhd,[10] although some research workers have developed an *in situ* preparation of this compound, starting with a variety of elemental sources including metallic Sr, Sr(OH)$_2$, SrO, and $SrCO_3$.[4,11,12] Additionally, the β-diketonate derivatives of group 2 elements are highly hygroscopic, and retain water with some tenacity.[13]

A further limiting factor in obtaining intense blue light emitting SrS:Ce is the lack of suitable cerium-containing dopant sources. The primarily utilized cerium precursor Ce(tmhd)$_4$[14] produces mainly green–blue emission. This effect occurs, in part, because of the large size of Ce(β-diketonate)$_4$ molecules with analogously encaged cerium cores,[15] as well as because of the potential of incorporation of oxygen impurities in the strontium sulfide host lattice, presumably due to incomplete cleavage of all existing cerium–oxygen bonds. Thus was the status of ALE of SrS:Ce for TFEL when the present investigation was undertaken. Specifically, one of the issues to address was whether the disadvantageous incorporation of oxygen adjacent to cerium emitters was the origin of the observed optical emission quenching in Ce(tmhd)$_4$ derived films, or whether it was due to an inhomogeneous incorporation profile, perhaps exacerbated by the large footprint of the dopant moiety on the substrate surface.

Ce{N[Si(CH$_3$)$_3$]$_2$}$_3$ has been prepared according to existing procedures[16] by reacting cerium(III) chloride and lithium hexamethyldisilylamide in THF [eqn. (1)].

$$CeCl_3 + 3\ Li\{N[Si(CH_3)_3]_2\} \rightarrow Ce\{N[Si(CH_3)_3]_2\}_3 + 3\ LiCl \quad (1)$$

Multiple sublimations yielded an extremely air- and moisture-sensitive yellow powder which was used in ALE experiments. It represents a highly volatile cerium compound, which was shown by thermogravimetric analysis to stay intact in the vapor phase (Fig. 3).

Suitable single crystals for X-ray diffraction were grown from a concentrated hexane solution, obtained by extraction

‡Fig. 2 indicates that both pK_{a1} and a pK_{a2} influence the ALE operation. The creation of a S–H terminated surface from a Sr(β-diketonate)$_2$ terminated surface relies on H_2S input and, here, pK_{a1} is the controlling feature. Likewise, the interactions of the resultant S–H terminated surface with additional metal–ligand complexes are dominated by pK_{a2}.

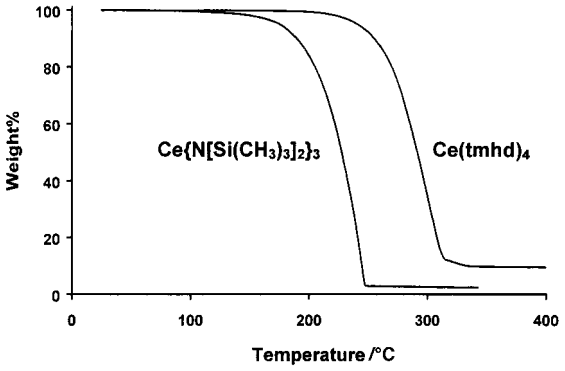

Fig. 3 TGA plots of Ce{N[Si(CH$_3$)$_3$]$_2$}$_3$ and Ce(tmhd)$_4$.

of the crude product with hexane and subsequent removal of lithium chloride. The crystal structure representation of the cerium tris(amide) compound is depicted in Fig. 4. It exhibits a three-coordinate central atom, isostructural with its Nd,[17] Yb,[18] Eu,[19] Sc,[19] Dy,[20] Er[20] and Pr[21] derivatives, surrounded by three nitrogen atoms. The cerium atom displays a disorder in the *z* direction, occupying two sites positioned 0.31 Å above and below the plane formed by the nitrogen atoms.

Ce{N[Si(CH$_3$)$_3$]$_2$}$_3$ has been employed, along with Ce(tmhd)$_4$, in ALE experiments as a dopant source for ALE growth of SrS. Preliminary results are compiled (Table 2). As can be viewed from Table 2, cerium dopants in SrS films which originate from cerium β-diketonates, when compared with those originating from cerium amides, emit visible electromag-

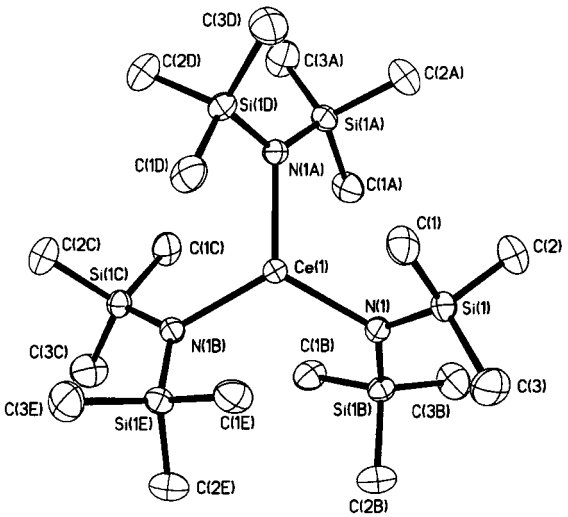

Fig. 4 Crystal structure representation of Ce{N[Si(CH$_3$)$_3$]$_2$}$_3$.

Table 2 Emission characteristics of SrS:Ce obtained employing Ce(tmhd)$_4$ and Ce{N[Si(CH$_3$)$_3$]$_2$}$_3$ as cerium dopant sources in ALE growth

Item	Ce(tmhd)$_4$	Ce{N[Si(CH$_3$)$_3$]$_2$}$_3$
λ_{max}/nm[a]	518	≈480
cd m^{-2}	28	9
x[a]	0.30	0.20
y	0.52	0.40
[1 cd m^{-2} + 50 v]B_{on}[b]	23–61	≈12–22
[1 cd m^{-2}]V_{thr}[c]	81 ± 2	75–112
[Ce]XRF(wt%)[d]	0.91–1.19	0.20–2.40
$\tau_{1/2}$[e]/ns	11–14	15–20

[a]1931 C.I.E. chromaticity diagram. [b]Emission determined to be 1 cd m^{-2}, and drive voltage increased 50 V above this point. [c]Threshold voltage. [d]Cerium concentration determined by X-ray fluorescence. [e]Emission half-life.

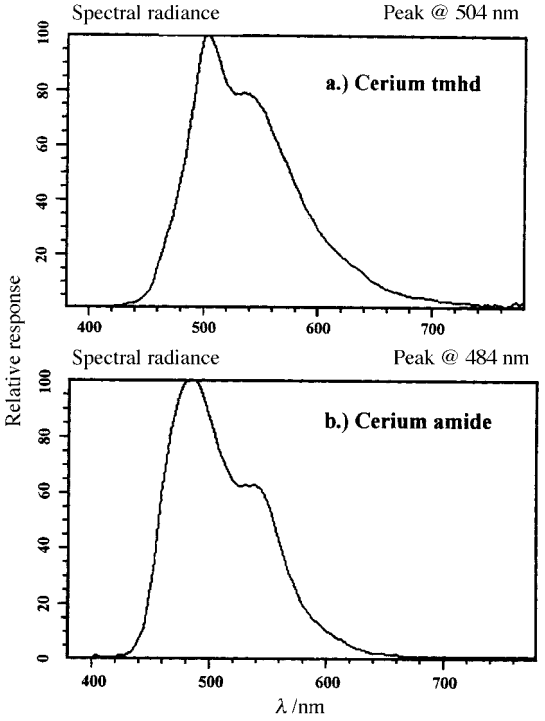

Fig. 5 Comparison of EL wavelength emissions for SrS:Ce doped with (a) $Ce(tmhd)_4$ and (b) $Ce\{N[Si(CH_3)_3]_2\}_3$.

netic radiation at a wavelength shifted almost 40 nm towards the blue region of the spectrum (Fig. 5). Additional efforts to improve emission intensity are underway and will be reported in due course. The shoulder observed in the emission spectra is consistent with the cerium manifold.[1] At this point, the wide range of [Ce] observed in the samples may be understood best as an accumulation in the front of the reaction zone, and a depletion towards the terminal end of that zone. This is consistent with the higher protolytic activity of the amide ligand towards the S–H terminated surface, as compared to the β-diketonate ligand.

A possible explanation for the observed wavelength shift lies in the difference of cerium–nitrogen and –oxygen bond strengths. Contrary to relatively stable Ce–O bonds, the extremely basic Ce–N linkages should ensure complete dissociation of the lanthanide core upon contact with protonated substrate surfaces. Comparison of the pK_{a2} of H_2S (11.96) with the pK_a of $H\{N[Si(CH_3)_3]_2\}$ (16.42),[22] clearly indicates that the dominant ALE process, protonation, should be facile. Furthermore, the values of 16.42 [$H\{N[Si(CH_3)_3]_2\}$ and 15.9 [Htmhd] provide support for the idea that the more basic amide ligand will be easier to protonate off of the cerium center in an ALE scheme, when compared to the examined β-diketone example. As may be understood by the spatial relationships existent between the Ce–L unit and near neighbor S–H groups, the footprint of the substrate-attached precursor (neutral molecule absent one ligand) substantially is larger for the β-diketonate originating species, relative to the amide counterpart. Examination of thermal desorption mass spectrometry data confirm that the substrate attachment mode for each precursor is consistent with this motif of binding.[23]

Conclusion

The traditional dopant precursor for ALE growth of SrS:Ce, $Ce(tmhd)_4$, provides a green side green–blue emission in a TFEL FPD. By replacing cerium–oxygen interactions in the precursor with cerium–nitrogen counterparts the level of oxygen incorporation in the films, as determined by SIMS, has been reduced.[24] It is surmised that one disadvantageous role of oxygen in these electronic materials is to decrease the emission lifetime, *via* excited state quenching, and, thereby, reduce the overall utility of the resultant film. Furthemore, by incorporating directly Ce^{3+} from the precursor, in the form of the amide, as opposed to the Ce^{4+}, found in the β-diketonate, the footprint of the surface-bound species has been reduced tremendously. Lastly, by reliance on a more basic ligand for the dopant atom, a precursor molecule which has been designed expressly for the ALE operational mode has been employed. By capitalizing upon the protonation chemistry which dominates the ALE scheme, dopant atom incorporation has been rendered a more facile process. Ultimately, the combination of reduced oxygen content, smaller footprint of surface bound dopant fragments, and reliance on a dopant molecule designed for the specifics of ALE have combined to produce a blue shift in the EL, to stimulate an increase in the emission lifetime, and, perhaps, to guide the direction for future design of molecules which are tailored to ALE of electronic materials.

Experimental

General considerations

Due to the extreme oxygen- and moisture-sensitivity of the synthesized cerium amide, all manipulations were carried out under a dried and purified argon atmosphere on a vacuum line by employing standard Schlenk or inert gas-filled glove box techniques. Solvents were degassed and freshly distilled from sodium– or potassium–benzophenone prior to use. The obtained compound has been characterized by single-crystal X-ray diffraction, satisfactory elemental analysis, thermogravimetric examination, as well as mass spectroscopy.

Instrumentation

The crystal structure of $C_{18}H_{54}CeN_3Si_6$ was determined using a Siemens SMART CCD diffractometer at 173 K. A suitable single crystal was selected under a microscope and mounted on the diffractometer under a continuous liquid-nitrogen cooled argon stream.

The low resolution mass spectrum was collected using a VG Instruments 70SE spectrometer with a 70 eV ion source, in a vacuum of 10^{-6} Torr, employing a direct insertion probe. Elemental analysis was conducted in an argon-sealed volatile sample pan using a Perkin Elmer Series II CHNS/O Analyzer. Thermogravimetric analysis was recorded employing a Perkin Elmer TGA7 instrument inside an inert atmosphere glove box. Lithium content was determined utilizing a Perkin-Elmer Optima 3000 ICP-OES Analyzer. Solutions of lithium chloride dissolved in *ca.* 15% nitric acid ranging from 10 to 0.0001 ppm were employed to calibrate the instrument. A cerium tris(amide) solution in *ca.* 15% nitric acid was prepared with an approximate cerium concentration of 1 ppm. The melting point of $Ce\{N[Si(CH_3)_3]_2\}_3$ was determined in a sealed capillary on a MELT-TEMP II apparatus, and is uncorrected.

Synthesis of $Ce\{N[Si(CH_3)_3]_2\}_3$

To a suspension consisting of 11.79 g (47.85 mmol) of anhydrous $CeCl_3$ in 100 mL of THF in a 500 mL Schlenk flask a solution of 24.01g (143.55 mmol) of lithium bis(trimethylsilyl)amide in 300 mL of THF was added dropwise through a cannula under reflux over a period of 5 h. After attaining ambient temperature on its own the yellow solution, with residual cerium chloride, was stirred overnight and subsequently reduced under vacuum to dryness. Following extraction by hexane and separation of lithium chloride by Schlenk filtration, the solvent was removed at reduced pressure and the crude reaction product was purified repeatedly by sublimation (100 °C/10^{-2} Torr) to remove unreacted lithium

Table 3 Atomic coordinates ($\times 10^4$) and equivalent isotropic displacement parameters ($Å^2 \times 10^3$) for $Ce\{N[Si(CH_3)_3]_2\}_3$. U_{eq} is defined as one third of the trace of the orthogonalized U_{ij} tensor

Atom	x	y	z	U_{eq}
Ce(1)	6667	3333	7874(1)	30(1)
N(1)	7480(1)	4959(2)	7500	26(1)
Si(1)	7138(1)	5494(1)	8894(1)	28(1)
C(1)	6341(2)	4566(2)	10362(4)	42(1)
C(2)	6454(3)	6010(3)	8001(4)	47(1)
C(3)	8133(3)	6435(3)	10063(4)	52(1)

Table 4 Selected interatomic distances (Å) and angles (°) for $Ce\{N[Si(CH_3)_3]_2\}_3$

Ce(1)–N(1)	2.320(3)	Ce(1)–N(1)–Si(1)	110.46(9)
N(1)–Si(1)	1.702(2)	N(1)–Si(1)–C(1)	107.40(14)
Si(1)–C(1)	1.870(3)	N(1)–Si(1)–C(2)	112.83(12)
Si(1)–C(2)	1.856(3)	N(1)–Si(1)–C(3)	113.77(14)
Si(1)–C(3)	1.855(3)	Si(1)–N(1)–Si(1)$^{\#1}$	127.2(2)

$^{\#1}$Symmetry operation used to generate the equivalent atom: $-x+y+1, y, -z+3/2$

amide. A dark yellow powder was obtained. Attempted crystallization from pentane and hexane did not result in crystals suitable for X-ray crystallography. Yield 5.13 g (17%); mp 159–161 °C; MS [EI, 70 eV, m/z (%), 251 °C]: 621 (25) $[M^+ + 1]$*, 605 (8) $[M^+ - CH_3]$,* 459 (74) $[M^+ - HN[Si(CH_3)_3]_2]$,* 444 (19) $[M^+ - HN[Si(CH_3)_3]_2 - CH_3]$,* 428 (5) $[M^+ - N[Si(CH_3)_3]_2 - 2CH_3]$,* 299 (47) $[M^+ - 2N[Si(CH_3)_3]_2 - H]$,* 146 (100) $[Si(CH_3)_3]_2^+$ (*Cerium isotopic pattern). [Found: C, 34.60; H, 8.92; N, 6.63. Calc. for $C_{18}H_{54}CeN_3Si_6$: C, 34.80; H, 8.76; N, 6.76. No lithium content was detected by the ICP technique (Inductively Coupled Plasma).

Crystal structure determination of $Ce\{N[Si(CH_3)_3]_2\}_3$

$C_{18}H_{54}CeN_3Si_6$, $M = 621.107$, trigonal, space group $P\bar{3}1c$ (no. 163), $a = 16.3243(4)$ Å, $c = 8.2873(2)$ Å, $V = 1912.55(8)$ Å^3, $T = 173(2)$ K, $Z = 2$, λ(Mo-Kα) = 0.71073 Å, $F(000) = 718$, crystal size $0.345 \times 0.286 \times 0.286$ mm (the crystal was measured using a calibrated reticle in a microscope), $\mu = 1.393$ mm^{-1}, 9822 reflections measured, 1130 unique ($R_{int} = 0.0290$), final R indices [$I > 2\sigma(I)$]: $R_1 = 0.0331$, $wR_2 = 0.0945$, R indices (all data): $R_1 = 0.0359$, $wR_2 = 0.0969$, refinement method: full-matrix least squares on F^2, goodness-of-fit 1.192, extinction coefficient 0.0085(14), largest difference peak and hole: 0.803 and -0.310 e Å^{-3}. An absorption correction using SADABS was applied. Hydrogen atoms were refined as HFIX from SHELXTL using an appropriate riding model with varied thermal parameters. After the structure was refined, two peaks of 2.58 and 2.42 e Å^{-3} remained occupying a general and a four-fold special position. When refined as carbon atoms, the R factor and residual electron density were reduced to the final values. The two peaks are arranged about a $\bar{3}$ position and are believed to be a disordered THF molecule. Their multipliers were adjusted (0.2333 and 0.6) to give two molecules per unit cell (*i.e.* 10 atoms total) with closest carbon–carbon contacts of 4.3 Å. No attempt was made to assign oxygen scattering factors or to locate hydrogen atoms. The disordered cerium atom lies 0.31 Å above and below the N_3 plane with site occupancies of 50% and 50% (0.5 and 0.5) actual multiplier 0.1666 (1/6), respectively. Full atomic coordinates with equivalent isotropic thermal parameters and selected interatomic distances and angles are compiled in Table 3 and 4, respectively. Full crystallographic details, excluding structure factors, have been deposited at the Cambridge Crystallographic Data Centre (CCDC). See Information for Authors, Issue 1. Any request to the CCDC for this material should quote the full literature citation and the reference number 1145/112.

We acknowledge gratefully the financial support of this project by DARPA and the Georgia Institute of Technology Molecular Design Institute. Planar International in Helsinki, Finland kindly provided assistance with the EL measurements. William S. Rees, Jr. is the recipient of an Alexander von Humboldt grant at TU Berlin for the period 1998–99.

References

1 C. N. King, *J. Vac. Sci. Technol.*, *A*, 1996, **14**, 1729.
2 P. D. Rack, P. H. Holloway, L. Pham, J. Wager, S.-S. Sun, E. Dickey and C. N. King, *SID 95 Digest*, 1995, 480.
3 M. Takeda, Y. Kanatani, H. Kishishita and H. Uede, *Proc. SPIE-Int. Soc. Opt. Eng.*, 1983, **34**, 386.
4 M. Tiitta and L. Niinistö, *Chem. Vap. Deposition*, 1997, **3**, 167.
5 T. Suntola, J. Antson, A. Pakkala and S. Lindfors, *SID 80 Digest*, 1980, 108.
6 W. S. Rees, Jr., in *CVD of Nonmetals*, Wiley-VCH, Weinheim, 1st edn., 1997, p. 254.
7 P. W. Atkins in *Physical Chemistry*, W. H. Freeman and Company, New York, 4th edn., 1990, p. 951.
8 H. Yokoi and T. Kishi, *Chem. Lett.*, 1973, 749.
9 D. J. Otway, H. A. Luten, K. M. A. Malik, M. B. Hursthouse and W. S. Rees, Jr., *Mater. Res. Soc. Symp. Proc.*, 1996, **415**, 105.
10 S. R. Drake, M. B. Hursthouse, D. J. Otway and K. M. A. Malik, *J. Chem. Soc.*, *Dalton Trans.*, 1993, 2883.
11 P. Soininen, E. Nykänen, L. Niinistö and M. Leskelä, *Chem. Vap. Deposition*, 1996, **2**, 69.
12 M. Leskelä, L. Niinistö, E. Nykänen, P. Soininen and M. Tiitta, *Thermochim. Acta*, 1991, **175**, 91.
13 D. J. Otway, H. A. Luten, O. Just and W. S. Rees, Jr., *Mater. Res. Soc. Symp. Proc.*, 1998, in press; D. J. Otway, H. A. Luten and W. S. Rees, Jr., *Mater. Res. Soc. Symp. Proc.*, 1996, **415**, 105; W. S. Rees, Jr., M. Carris and W. Hesse, *Inorg. Chem.*, 1991, **30**, 4479.
14 E. Uhlemann and F. Dietze, *Z. Anorg. Allg. Chem.*, 1971, **386**, 329.
15 M. Leskelä, R. Silanpää, L. Niinistö and M. Tiitta, *Acta Chem. Scand.*, 1991, **45**, 1006.
16 D. C. Bradley, J. S. Ghotra and F. A. Hart, *J. Chem. Soc.*, *Dalton Trans.*, 1973, 1021.
17 R. A. Andersen, D. H. Templeton and A. Zalkin, *Inorg. Chem.*, 1978, **17**, 2317.
18 P. G. Eller, D. C. Bradley, M. B. Hursthouse and D. W. Meek, *Coord. Chem. Rev.*, 1977, **24**, 1.
19 J. S. Ghotra, M. B. Hursthouse and A. J. Welch, *J. Chem. Soc.*, *Chem. Commun.*, 1973, 669.
20 W. A. Herrmann, R. Anwander, F. C. Munck, W. Scherer, V. Dufaud, N. W. Huber and G. R. J. Artus, *Z. Naturforsch.*, *Teil B*, 1994, **49**, 1789.
21 W. S. Rees, Jr., O. Just and D. S. Van Derveer, unpublished work.
22 Y. V. Kolodyazhnyi, M. G. Gruntfest, N. I. Sizowa, A. P. Sadimenko, L. I. Ol'khovskaya and N. V. Komarow, *Zh. Obshch. Khim.*, 1983, **53**, 678.
23 W. S. Rees, Jr., O. Just, A. Kaloyeros and G. Peterson, unpublished work.
24 W. S. Rees, Jr., O. Just, B. Pathengy, P. Holloway, E. Soininen and R. Tornqvist, unpublished work.

Paper 8/05757E